pharmaceuticals

Article

Vemurafenib Inhibits Enterovirus A71 Genome Replication and Virus Assembly

Bodan Hu [1,†], Kenn Ka-Heng Chik [1,2,†], Jasper Fuk-Woo Chan [1,2,3,†], Jian-Piao Cai [1], Hehe Cao [1], Jessica Oi-Ling Tsang [1,2], Zijiao Zou [1], Yin-Po Hung [1], Kaiming Tang [1], Lilong Jia [1], Cuiting Luo [1], Feifei Yin [3,4], Zi-Wei Ye [5], Hin Chu [1,2], Man-Lung Yeung [1,2] and Shuofeng Yuan [1,2,*]

1 State Key Laboratory of Emerging Infectious Diseases, Carol Yu Centre for Infection, Department of Microbiology, School of Clinical Medicine, Li Ka Shing Faculty of Medicine, The University of Hong Kong, Pokfulam, Hong Kong SAR, China
2 Centre for Virology, Vaccinology and Therapeutics, Hong Kong Science and Technology Park, Hong Kong SAR, China
3 Hainan Medical University-The University of Hong Kong Joint Laboratory of Tropical Infectious Diseases, Hainan Medical University, Haikou 571199, China
4 Key Laboratory of Tropical Translational Medicine of Ministry of Education, Hainan Medical University, Haikou 571199, China
5 School of Biomedical Sciences, Li Ka Shing Faculty of Medicine, The University of Hong Kong, Pokfulam, Hong Kong SAR, China
* Correspondence: yuansf@hku.hk
† These authors contributed equally to this work.

Abstract: Enterovirus A71 (EV-A71) infection is a major cause of hand, foot, and mouth disease (HFMD), which may be occasionally associated with severe neurological complications. There is currently a lack of treatment options for EV-A71 infection. The Raf-MEK-ERK signaling pathway, in addition to its critical importance in the regulation of cell growth, differentiation, and survival, has been shown to be essential for virus replication. In this study, we investigated the anti-EV-A71 activity of vemurafenib, a clinically approved B-Raf inhibitor used in the treatment of late-stage melanoma. Vemurafenib exhibits potent anti-EV-A71 effect in cytopathic effect inhibition and viral load reduction assays, with half maximal effective concentration (EC_{50}) at nanomolar concentrations. Mechanistically, vemurafenib interrupts both EV-A71 genome replication and assembly. These findings expand the list of potential antiviral candidates of anti-EV-A71 therapeutics.

Keywords: enterovirus; vemurafenib; RAF; MAPK signaling pathway; genome replication; virus assembly; VP0 cleavage

Citation: Hu, B.; Chik, K.K.-H.; Chan, J.F.-W.; Cai, J.-P.; Cao, H.; Tsang, J.O.-L.; Zou, Z.; Hung, Y.-P.; Tang, K.; Jia, L.; et al. Vemurafenib Inhibits Enterovirus A71 Genome Replication and Virus Assembly. *Pharmaceuticals* **2022**, *15*, 1067. https://doi.org/10.3390/ph15091067

Academic Editor: Zoidis Grigoris

Received: 26 July 2022
Accepted: 25 August 2022
Published: 27 August 2022

1. Introduction

Enterovirus A71 (EV-A71) infection is a major cause of hand, foot, and mouth disease (HFMD), which can be associated with life-threatening neurological complications, such as encephalitis, meningitis, and poliomyelitis-like syndrome [1]. Since its first isolation in 1969 in California, EV-A71 has been recognized as a serious health threat, especially to infants and young children, and has caused major outbreaks in the Asia-Pacific region [1,2]. Despite its clinical importance, there is a lack of treatment options for EV-A71 infection [3].

EV-A71 belongs to the genus Enterovirus of the *Picornaviridae* family. The genus contains various important human pathogens, such as coxsackieviruses, rhinoviruses, echoviruses, and numbered enteroviruses [4]. Enteroviruses are non-enveloped viruses with a single-stranded positive-sensed RNA genome surrounded by the capsid composed of VP0-VP4 [1]. The replication cycle of enteroviruses starts with binding to their receptors, such as scavenger receptor class B member 2 (SCARB2), human tryptophanyl-tRNA synthetase (hWARS), and P-selectin glycoprotein ligand 1 (PSGL1) [4,5]. After entering the host cells through endocytosis, the virions undergo the uncoating process with deformation of

capsid proteins and release viral RNA genome into cytoplasm [6]. The genomic replication and transcription take place in virus-induced membrane replication organelles [7]. Following the synthesis of viral proteins and proteolytic processing by viral protease $3CD^{pro}$, assembly of progeny virions occurs through self-oligomerization of capsid proteins VP0, VP1, and VP3 into protomers and pentamers [8,9]. Incorporation of nascent genome RNA into capsid induces the cleavage of VP0 into VP2 and VP4, generating mature and infectious progeny virions [10,11].

Viruses can manipulate host machinery to regulate host antiviral responses and facilitate viral replication. The RAF-MEK-ERK pathway, one of the three mitogen-activated protein kinases (MAPK) cascades, plays an important role in the regulation of cell proliferation, differentiation, and apoptosis [12]. The kinase signaling pathway is induced by extracellular agents including both DNA and RNA viruses [13]. Aberrant regulation takes place during infection of various viruses, such as influenza virus, hepatitis C virus, coxsackievirus, Ebola virus, and coronaviruses [13–16]. Inhibition of the MAPK/ERK pathway leads to retention of viral ribonucleoproteins (RNPs) of influenza viruses in the cell nucleus and impairs viral replication [14].

Enteroviruses such coxsackievirus B3 and EV-A71 induce a biphasic activation of the MAPK/ERK signaling pathway immediately after virus binding to receptors and in the late stage of infection [16,17]. ERK pathway inhibitors and siRNA against ERK inhibit EV-A71 infection [18]. EV-A71-induced ERK signaling activation may promote cyclooxygenase-2 expression, one of the factors contributing to neurological inflammation during infection [19]. Therefore, targeting the RAF-MEK-ERK pathway may be a useful therapeutic strategy for EV-A71 infection.

Drug repositioning has been increasingly applied to identify potential therapeutics for viral infections [20,21]. It has several potential advantages over de novo drug development, such as significant reduction in cost and time due to known safety and pharmacokinetics data, and an increase in drug approval rates. Therefore, we employed the drug repositioning strategy to investigate whether vemurafenib, an FDA-approved RAF inhibitor for treating $BRAF^{V600}$ mutant-related melanoma, could be used for the treatment of EV-A71 infection. Vemurafenib selectively inhibits the activating $BRAF^{V600}$ mutant kinase to block the downstream BRAF-MEK-ERK signaling transduction. In turn, it reduces aberrant melanoma cell proliferation, promoting cell apoptosis [22,23]. We showed that vemurafenib potently inhibits EV-A71 in vitro and activates the MAPK/ERK kinase cascades and restricts virus genome replication and virus assembly.

2. Results

2.1. Vemurafenib Potently Inhibits EV-A71 Infection

To investigate whether vemurafenib possesses an antiviral activity against EV-A71, we first conducted a cytopathic effect (CPE) inhibition assay to assess vemurafenib's ability to inhibit virus-induced CPE formation in human rhabdomyosarcoma (RD) cells. As shown in Figure 1A,B, vemurafenib dose-dependently inhibited EV-A71-induced CPE in RD cells, with half maximal effective concentration (EC_{50}) and 50% cytotoxicity concentration (CC_{50}) of 0.34 ± 0.01 μM and 17.71 ± 0.58 μM, respectively. In the viral load reduction assay, vemurafenib also demonstrated a dose-dependent inhibitory effect against EV-A71 (Figure 1C). The antiviral activity of vemurafenib was similar to that of the broad-spectrum viral polymerase inhibitor remdesivir, which is known to be active against EV-A71, SARS-CoV-2, and other RNA viruses [24–26]. Importantly, the selectivity index of vemurafenib (52.1) was even higher than that of remdesivir (35.5), indicating the potential of vemurafenib as a repositioned drug for EV-A71 infection.

2.2. Time-of-Drug-Addition of Vemurafenib on EV-A71 Infection

To explore which stage(s) of EV-A71 life cycle is targeted by vemurafenib, we performed a time-of-drug-addition assay [27], in which RD cells were treated with vemurafenib at different time points before, concurrently with, or after virus infection (Figure 2A).

One cycle of EV-A71 replication is usually finished within 6–8 h [28,29]; therefore, we collected samples for analysis 10 h after infecting cells at a high multiplicity of infection (MOI = 1). There was a significant reduction in titers of progeny virions in the culture supernatant when RD cells were subjected to treatment at either before (−1 h), concurrently with (0 h), or at latest 4 h after infection, and the reduction was more prominent with earlier treatment (Figure 2B). Vemurafenib exhibited no inhibitory effect when the infected cells were treated at 6 or 8 h post-infection (hpi). To further characterize the antiviral activity of vemurafenib, we analyzed viral RNA synthesis and protein translation in cells. As shown in Figure 2C, cellular viral load also decreased with drug addition at earlier time points. The inhibition was evident even when vemurafenib was added at 6 hpi or 8 hpi, and a similar pattern of gradual decrease in antiviral activity was noted. Indirect immunofluorescence assay showed that EV-A71 VP1 protein expression was also affected (Figure 2D). Altogether, these results suggested that vemurafenib does not function as an entry inhibitor or target viral functional proteins such as protease or polymerase. Instead, it likely induces changes in host cells to impair viral genome replication and transcription, resulting in reduced viral protein translation.

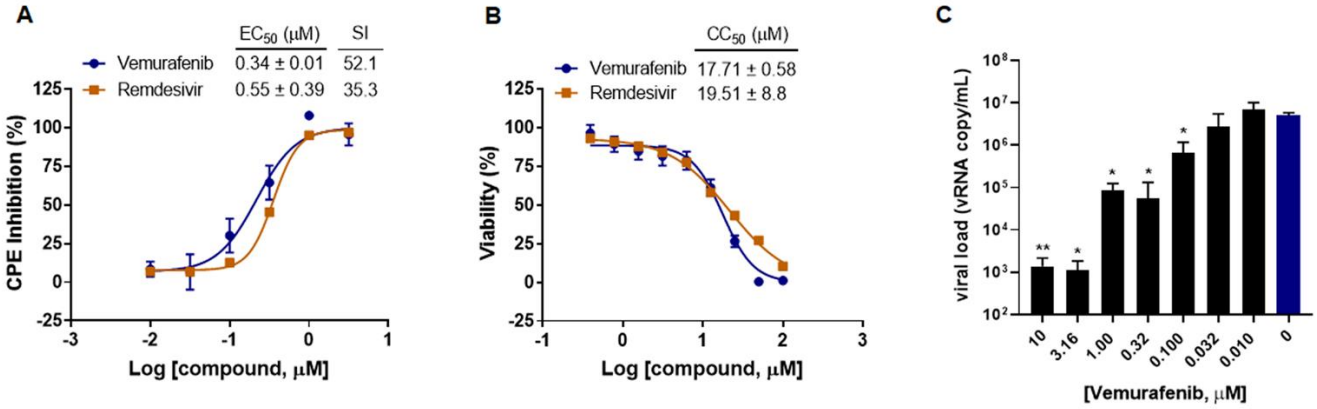

Figure 1. Vemurafenib significantly inhibits EV-A71 infection. (**A**) EV-A71 infection (MOI = 0.01) induced CPE inhibition by and (**B**) cytotoxicity of vemurafenib and remdesivir (as a control) in RD cells. (**C**) Viral load in the culture supernatant at the presence of serially diluted vemurafenib. Data are representative of three independent experiments and displayed as means ± standard deviation. Asterisks (*) indicate statistically significant differences (** $p < 0.01$ and * $p < 0.05$, Student's *t*-test) between vemurafenib treatment and mock treatment (0 μM, colored in blue). EC_{50} and CC_{50} were obtained with non-linear regression analysis. EC_{50}: half maximal effective concentration to completely inhibit EV-A71 infection. CC_{50}: 50% cytotoxic concentration. SI: selective index, CC_{50}/EC_{50}.

2.3. Virus Assembly Was Impaired with Vemurafenib Treatment

At the later stages of EV-A71 life cycle, viral structural capsid proteins, VP0, VP1, and VP3, assemble into heterotrimeric protomers and then pentamers to initiate assembly of progeny virions [8,10,11]. The subsequent VP0 cleavage into VP2 and VP4 is a critical step to generate fully mature virions [8]. To investigate whether the assembly of EV-A71 is affected by vemurafenib, we analyzed the amount of VP2 relative to VP0 when infection was performed in the presence of vemurafenib at a concentration that did not completely inhibit virus replication. As shown in Figure 3A, at low MOI of 0.01, virions produced under the pressure of vemurafenib have less VP2 than those treated with DMSO. The successfully cleaved product VP2 in the virions produced in the presence of vemurafenib was only ~50% of those treated with DMSO (Figure 3B). The defect is even more obvious when infection was performed at a high MOI of 1, in which it takes shorter time until all cells die of infection. A very faint band corresponding to VP2 was observed, whereas VP1 and VP0 were easily detected (Figure 3C). Taken together, these results indicated that the VP0 cleavage during virus assembly is disturbed when vemurafenib is added as an antiviral drug.

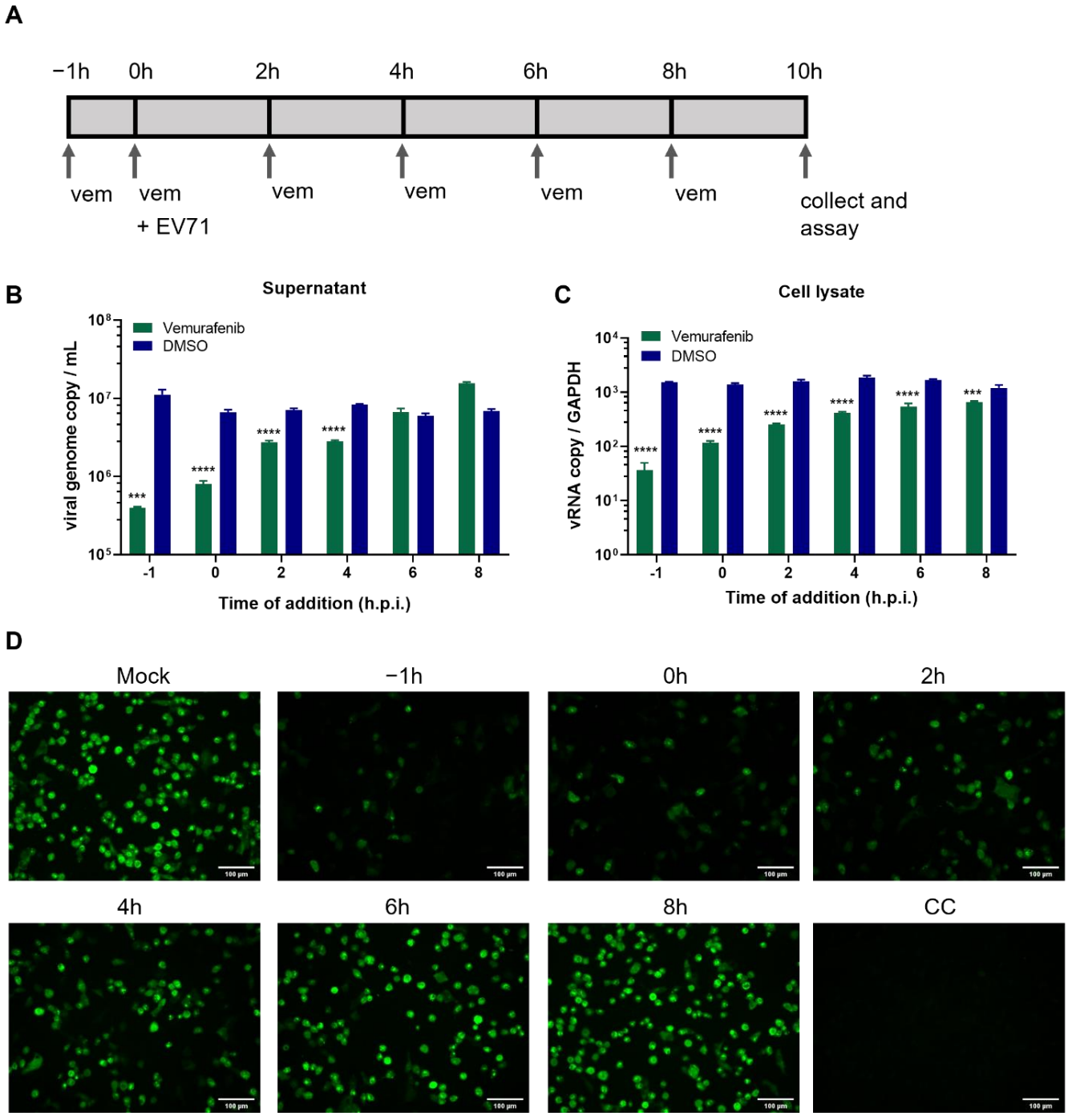

Figure 2. The time-of-drug-addition assay with vemurafenib. RD cells were infected with EV-A71 at an MOI of 1, and treated with 2 μM vemurafenib at varied time points, including pre-infection (−1 h), co-infection (0 h), and post-infection (2 h, 4 h, 6 h, or 8 h). (**A**) Graphical scheme illustrating the experimental design. (**B**) The amount of viral RNA released into culture supernatant, measured by real-time RT-PCR using primer targeting 5′-UTR. (**C**) The relative amount of viral genome RNA in the cells. Data are representative of three independent experiments. Asterisks (*) indicate statistically significant differences (*** $p < 0.001$, **** $p < 0.0001$) between vemurafenib and DMSO according to a Student's *t*-test. (**D**) VP1 expression detected by indirect immunofluorescence. Mock: mock treatment, RD cells were infected EV-A71 but without vemurafenib treatment. CC: mock infection, RD cells only, without infection nor vemurafenib treatment. Scale bar equals to 100 μm. Representative images are shown.

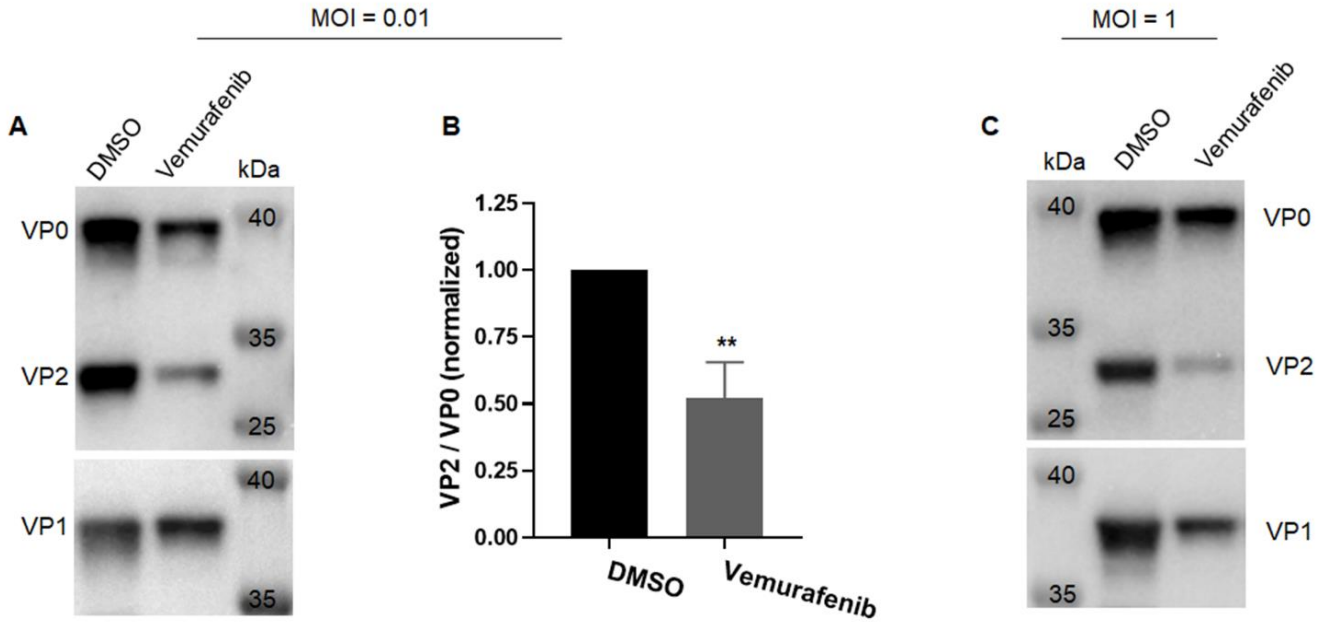

Figure 3. Virus assembly is impaired with vemurafenib treatment. (**A**,**B**) RD cells were infected with EV-A71 at an MOI of 0.01 and concurrently treated with 1 μM vemurafenib or 0.005% DMSO. Viruses in culture supernatant were pelleted through 20% sucrose cushion and subjected to western blot. VP0 and VP2 were detected with anti-VP2 antibody. VP1 was detected using anti-VP1 antibody. (**A**) The amount of VP0, VP2, and VP1 in purified viruses. (**B**) Quantification of relative amount of VP2 to VP0. Density of VP0 and VP2 bands was determined and the VP2/VP0 ratio was calculated and normalized to that treated with DMSO. Results from three virus preparations are displayed as means ± standard deviation. Asterisks (*) indicate statistically significant differences (** $p < 0.01$) between DMSO mock treatment group and vemurafenib-treated group according to a Student's *t*-test. (**C**) The amount of VP0, VP2, and VP1 in purified viruses. RD cells are infected with EV-A71 at an MOI of 1 and concurrently treated with 2 μM vemurafenib or 0.01% DMSO. One representative result from two different virus preparation is shown.

2.4. RAF-MEK-ERK Signaling Pathway Was Activated by Vemurafenib

Vemurafenib is used for treatment of $BRAF^{V600}$ mutant metastatic melanoma. It highly selectively inhibits $BRAF^{V600}$ mutation-induced activation of the RAF-MEK-ERK signaling pathway, thus stopping cell proliferation and promoting apoptosis of $BRAF^{V600}$ melanoma cells. Mutant BRAF inhibitors have been shown to activate this MAPK kinase cascade in wild-type BRAF cells [30,31], which is also activated by EV-A71 infection [17,18]. Therefore, we investigated the RAF-MEK-ERK kinase responses to vemurafenib in RD cells alone or together with EV-A71 infection. Western blot showed that under normal conditions without virus infection, vemurafenib induces activation of the RAF-MEK-ERK kinase cascade as evident by increased phosphorylated MEK1/2 and ERK1/2 (Figure 4). The activation started as early as 2 h after treatment and persisted for at least 8 h. We also compared the effect of vemurafenib on cells with or without EV-A71 infection. Surprisingly, similar levels of phosphorylated MEK and ERK were detected (lane 2 vs lane 4 at each time point), indicating that EV-A71 had no additional effect on inducing MAPK/ERK kinase cascade at these time points. We additionally analyzed the activation of MEK-ERK kinase signaling at earlier time points, i.e., 15 min, 30 min, and 60 min, p.i., of EV-A71 infection. The results in Figure S1 showed that vemurafenib treatment caused general but less significant increase in phosphorylation of MEK1/2 and ERK1/2, regardless of EV-A71 infection or not. These observations indicate that vemurafenib induces a rapid activation of RAF/MEK/ERK kinase cascade, and the effect is more prominent with long-time treatment. Altogether, the intrinsic property of vemurafenib to activate the RAF/MEK/ERK kinase cascade can potentially interfere with later stages of EV-A71 replication.

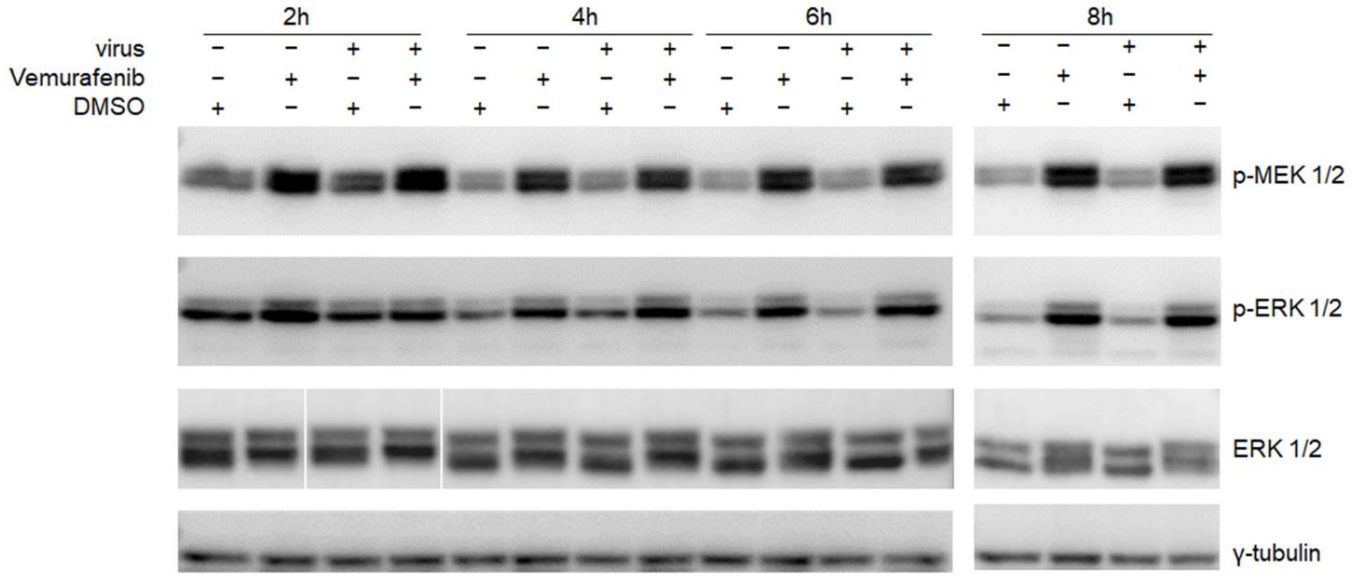

Figure 4. RAF-MEK-ERK kinase cascade was activated by vemurafenib treatment. RD cells were infected without or with EV-A71 at an MOI of 5 and concurrently treated with 4 μM vemurafenib or 0.02% DMSO. Cells were collected at 2 h, 4 h, 6 h, or 8 h post infection. Activation of RAF-MEK-ERK kinase cascade was analyzed by western blot. Phosphorylated MEK1/2 and ERK1/2 were detected using anti-phospho-MEK1/2 (Ser217/221) antibody and anti-phospho-ERK1/2 (Thr185/187) antibody. Unphosphorylated ERK and γ-tubulin were also detected as controls. Blots are representative data of two independent experiments.

3. Discussion

In this study, we repositioned the clinically available vemurafenib as a potential anti-EV-A71 therapeutic. Our results showed that vemurafenib potently inhibits EV-A71 in vitro, with an EC_{50} value in the nanomolar range. Previous studies showed that vemurafenib limits influenza A virus replication in A549 and calu-3 cells and inhibits human echovirus 1 infection in A549 cells, suggesting that vemurafenib or targeting MAPK kinase cascade could be a broad-spectrum antiviral strategy [32,33]. Vemurafenib is a drug approved for treatment of both adult and pediatric patients with unresectable or metastatic melanoma with the $BRAF^{V600}$ mutation [22,34,35]. Despite that the drug functions as a competitive inhibitor to block activation of the RAF-MEK-ERK signaling pathway in cells with mutant BRAF, we found that this inhibitor constantly activates the RAF signaling in RD cells which have a wild-type BRAF. The activation is more prominent with long-time treatment, and it is negligible at early time points of EV-A71 infection. The hyperactivation of RAF-MEK-ERK kinase cascade by vemurafenib has also been reported in a study on influenza A virus infection [33]. Vemurafenib activates CRAF in wild-type BRAF cells and the subsequent MEK/ERK phosphorylation [23,30,31]. Vemurafenib inhibits the activation of influenza A virus- or tumor necrosis factor alpha (TNFα)-induced JNK and p38 kinase signaling cascades, and the other two MPAK signaling pathways [12,33]. EV-A71 infection leads to activation of Jun-N-terminal kinase 1/2 (JNK1/2) [36] and induction of proinflammatory cytokines regulated by the MAPK p38 signaling cascades [37], thus regulating cell apoptosis and inflammation. Therefore, vemurafenib probably also limits the activation of the two MAPK signaling cascades induced by EV-A71, which may contribute to its inhibition of EV-A71 infection.

Given the complexity of the MAPK pathway and the fact that there are over 100 proteins involved in the downstream of ERK activation [12], activated ERKs induced by vemurafenib may target downstream proteins that are different from those induced by EV-A71 infection. In normal cells, activated ERKs are translocated to the cell nucleus and transactivate transcription factors to stimulate genes to promote cell mitosis and growth [12]. Furthermore, inhibition of RAF-MEK-ERK signaling impairs nuclear export of viral ri-

bonucleoprotein complexes (RNPs) of influenza A viruses which exploits cell nucleus for genome replication [14]. However, EV-A71 replication happens in a virus-induced unique replication organelle instead of cell nucleus [7]. The ROs formation is aided by host proteins including phosphatidylinositol 4-kinase-β (PI4KB) and oxysterol-binding protein (OSBP) [4,38]. Thus, the strategy of EV-A71 used for genome replication should be different from that used by influenza A viruses or host cell proliferation. On the other hand, EV-A71 infection-induced MAPK activation has been shown to cross talk with TNF-α-related cell apoptosis with the TNF-α induction appearing to be suppressed by ERK signaling to inhibit extrinsic apoptosis in EV-A71-infected cells [37]. The activated ERK signaling also interferes with the NF-kB pathway to upregulate expression of proinflammatory cytokines IL-6 and IL-8 and, more importantly, to increase viral replication [37]. Our results revealed that EV-A71 genome replication is impaired by vemurafenib treatment, and earlier addition of inhibitor leads to more severe defect. Altogether, it would support the hypothesis that vemurafenib competes with EV-A71 to activate MAPK/ERK pathway to promote gene expression for cell growth in the nucleus, which fails to provide support, e.g., PI4KB, for EV-A71 ROs formation and genome replication. The detailed involvement of the MAPK signaling pathway with ROs formation should be further investigated.

A crucial step in virions maturation is VP0 cleavage into VP2 and VP4. We also found that vemurafenib treatment led to reduced VP2 production, indicating a defect in virus assembly. The VP0 cleavage is potentially mediated by incorporation of viral genome RNA into capsid [4,10]. Therefore, the impaired viral genome replication caused by vemurafenib might be responsible for the affected VP0 cleavage. However, the exact mechanism underlying VP0 cleavage remains poorly understood. Other host factors such as sterile alpha motif and histidine-aspartic acid domain-containing protein 1 (SAMHD1) and heat shock protein-90-beta (Hsp90β) are also involved in this process [29,39]. A link between MAPK signaling and SAMHD1 or Hsp90β requires further exploration.

In conclusion, vemurafenib demonstrates antiviral activity against EV-A71 infection. It induces RAF-MEK-ERK signaling in wild-type BRAF cells, potentially to promote cell mitosis and proliferation, which paradoxically impairs viral genome replication and virus assembly. Our findings provide new insights for developing antiviral inhibitors targeting the MAPK signaling pathway as a potential broad-spectrum antiviral strategy. Nevertheless, the complexity of the kinase cascade should be carefully examined to restrict potential host toxicity and side effects.

4. Materials and Methods

4.1. Cells, Viruses, and Reagents

Human rhabdomyosarcoma (RD, ATCC, CCL-136™) cells were maintained in Dulbecco's Modified Eagle's Medium (DMEM, Gibco, Waltham, MA, USA) supplemented with 10% heat-inactivated fetal bovine serum (FBS, Gibco, Waltham, MA, USA), 100 units/mL of penicillin and 1000 μg/mL of streptomycin (Gibco, Waltham, MA, USA) as previously described [40]. Human EV-A71 viruses (isolate MY104-9-SAR-97, GenBank: DQ341368) were cultured in RD cells in serum-free DMEM supplemented with 2% FBS. Virus stocks were stored at −80 °C and were titrated by a 50% tissue culture infection dose (TCID50) assay as previously described [41]. Vemurafenib (PLX4032) and remedesivir (GS-5734) were purchased from MedChemExpress (MCE) and dissolved in dimethylsulfoxide (DMSO) to prepare 20 mM stock.

4.2. Virus Inhibition Assay

The EV-A71 CPE inhibition assay was performed as previously described with slight modifications [27]. Briefly, the drug compounds were three-fold serially diluted with serum-free DMEM and added to confluent RD cells in 96-well culture plates (30,000 cells/well) in triplicate for 1 h at 37 °C. After incubation, the drug-containing media were removed, and EV-A71 (MOI of 0.01) was added together with fresh drug-containing media to each well. After adsorption for 1 h at 37 °C, the virus-compound mixture was removed, and the

cells were washed with DMEM once to remove unbound virus. Subsequently, media with antiviral compounds were added to the cells for further incubation for 24–48 h at 37 °C in 5% CO_2. To analyze inhibition of cytopathic effect (CPE), 50 µL of Promega cell-titer glo was added to each well 48h post infection and luminescence was then measured by Promega plate reader. To analyze virus yields in culture supernatant and virus genome replication in cells, culture supernatant (48 hpi) and cells were harvested (24 hpi) for analysis. Viral RNA was extracted using RNeasy Mini Kit (Qiagen, Hilden, Germany) according to the manufacturer's instruction and subjected to real-time RT-PCR using One Step TB Green® PrimeScript™ RT-PCR Kit II (TaKaRa) with primers targeting 5′-UTR of viral genome (forward primer: 5′- GCCCCTGAATGCGGCTAAT -3′, reverse primer: 5′- ATTGTCACCATAAGCAGCCA -3′). Cellular relative gene expression was normalized to GAPDH internal control (forward primer: 5′-GCCTCTTGTCTCTTAGATTTGGTC-3′, reverse primer: 5′-TAGCACTCACCATGTAGTTGAGGT-3′).

4.3. Time-of-Drug-Addition Assay

A Vemurafenib time-of-addition assay was performed as previously described with minor modifications [27]. Briefly, RD cells were seeded into 24-well plates (200,000 cells/well) or 8-well chamber slides (65,000 cells/well) one day before infection with EV-A71 at an MOI of 1. After adsorption for 1h, cells were washed once and changed to fresh media. Vemurafenib (2 µM) was added to the media at different time point (−1 h, 0 h, 2 h, 4 h, 6 h or 8 h) after inoculation. For the time point of "−1 h", RD cells were preincubated with vemurafenib for 1h before infection, and the compound was kept in the fresh media afterwards. For the time point of "0 h", vemurafenib was added together with EV-A71 inoculation and kept in the fresh media afterwards. Culture supernatant and cells were harvested at 10 hpi, and viral genome copy numbers were determined. To analyze VP1 expression, cells in the 8-well chamber slides were fixed after infection for 10 h, permeabilized, blocked, and then stained with in-house produced primary anti-VP1 antibody and anti-mice secondary antibody Alexa Fluor 488. Images were taken with Olympus BX53 equipped with an LED illuminator.

4.4. Virus Assembly Assay

RD cells in T175 flask were ~90–100% confluency and infected with EV-A71 at an MOI of 0.01 or 1. Vemurafenib (or DMSO) was added to the media after adsorption for 1 h. Culture media was harvested when over 50% cells showed CPE. After clearing cell debris by low-speed centrifugation (4000× *g*, 5 min), viruses were pelleted by ultracentrifugation (175,000× *g*, 1.5 h) through 20% sucrose cushion and resuspended in 1×TNE buffer (10 mM Tris, 100 mM NaCl und 1 mM EDTA, pH 7.4) as previously described [42], and then subjected to western blot analysis.

4.5. Western Blot

To analyze virus assembly, pelleted viruses were mixed with loading buffer containing β-mercaptoethanol, separated by SDS-PAGE, and blotted onto polyvinylidene difluoride (PVDF) membranes. In-house mouse monoclonal antibodies targeting VP2 and VP1 were used to detect both VP0 and VP2, and VP1, respectively.

To analyze the activation of MAPK pathway, RD cells were infected without or with EV-A71 at an MOI of 5 and concurrently treated with 4 µM vemurafenib or 0.02% DMSO for 1 h. Cells were then washed once with DMEM and replenished with serum-free DMEM. Cells were collected at varied time points (15 min, 30 min, and 60 min, 2 h, 4 h, 6 h, and 8 h) post-infection and lysed in radioimmunoprecipitation assay buffer (RIPA buffer, ThermoFisher, Waltham, MA, USA) supplemented with protease and phosphatase inhibitors (#A32961, ThermoFisher, Waltham, MA, USA). Proteins in cell lysates were separated by SDS-PAGE and blotted onto PVDF membranes. Phospho-MEK1/MEK2 (Ser217, Ser221) Monoclonal Antibody (#MA5-15016, Invitrogen, Waltham, MA, USA) and Phospho-ERK1/ERK2 (Thr185, Tyr187) Polyclonal Antibody (#44-680G, Invitrogen) were

used to detect phosphorylated MEK and ERK. P44/p42 MAPK (ERK 1/2) antibody (cell signaling, #9102) was used to detect endogenous level of total ERK 1/2 protein. Antibodies targeting γ-tubulin was purchased from Sigma (#T6557).

After washing away unbound primary antibodies, secondary antibody coupled with horseradish peroxidase (HRP) were incubated with membranes. Immobilon classico western HRP substrate (Millipore, Burlington, MA, USA) was applied to membrane to give chemiluminescence signals which was then detected by chemiluminescence imaging system (Alliance Q9, Uvitec, St. John's, NL, Canada). The density of bands was measured by Image J.

4.6. Statistical Analysis

Statistical comparisons between different groups were performed by Student's *t*-test using GraphPad Prism 8. $p < 0.05$ was considered statistically significant.

Supplementary Materials: The following are available online at https://www.mdpi.com/article/10.3390/ph15091067/s1, Figure S1: Responses of RAF-MEK-ERK kinase cascade to vemurafenib treatment at earlier time points of EV-A71 infection.

Author Contributions: Conceptualization, B.H., J.F.-W.C. and S.Y.; methodology, B.H., K.K.-H.C. and S.Y.; investigation, B.H., K.K.-H.C., J.F.-W.C., J.-P.C., H.C. (Hehe Cao), J.O.-L.T., Z.Z., Y.-P.H., K.T., L.J., C.L., F.Y., Z.-W.Y., H.C. (Hin Chu), M.-L.Y. and S.Y.; validation, B.H., K.K.-H.C. and S.Y.; resources, J.F.-W.C., M.-L.Y. and S.Y.; writing—original draft preparation, B.H.; writing—review and editing, K.K.-H.C., J.F.-W.C. and S.Y.; supervision, J.F.-W.C. and S.Y.; funding acquisition, J.F.-W.C., M.-L.Y. and S.Y. All authors have read and agreed to the published version of the manuscript.

Funding: This research was partly supported by the Health and Medical Research Fund (CID-HKU1-11, CID-HKU1-7 and 19180502), the Food and Health Bureau, The Government of the Hong Kong Special Administrative Region; Health@InnoHK, Innovation and Technology Commission, the Government of the Hong Kong Special Administrative Region; the Consultancy Service for Enhancing Laboratory Surveillance of Emerging Infectious Diseases and Research Capability on Antimicrobial Resistance for Department of Health of the Hong Kong Special Administrative Region Government; the Major Science and Technology Program of Hainan Province (ZDKJ202003); the research project of Hainan Academician Innovation Platform (YSPTZX202004); the Hainan Talent Development Project (SRC200003); HKU Seed Fund for Basic Research (202011159023 and 202111159088); the University of Hong Kong Outstanding Young Researcher Award; the University of Hong Kong Research Output Prize (Li Ka Shing Faculty of Medicine); donations from the Shaw Foundation Hong Kong, Richard Yu and Carol Yu, Michael Seak-Kan Tong, May Tam Mak Mei Yin, Lee Wan Keung Charity Foundation Limited, Providence Foundation Limited (in memory of the late Lui Hac Minh), Hui Ming, Hui Hoy and Chow Sin Lan Charity Fund Limited, Chan Yin Chuen Memorial Charitable Foundation, Marina Man-Wai Lee, the Hong Kong Hainan Commercial Association South China Microbiology Research Fund, and Lo Ying Shek Chi Wai Foundation; Research Grants Council, Early Career Scheme (27117419) and General Research Fund (17121620); and the Collaborative Research Fund (C4033-19E). The funding sources had no role in the study design, data collection, analysis, interpretation, or writing of the report.

Institutional Review Board Statement: Not applicable.

Informed Consent Statement: Not applicable.

Data Availability Statement: Data is contained within the article and supplementary material.

Conflicts of Interest: J.F.-W.C. received travel grants from Pfizer Corporation Hong Kong and Astellas Pharma Hong Kong Corporation Limited, and was an invited speaker for Gilead Sciences Hong Kong Limited and Luminex Corporation. The other authors declared no conflict of interests. The funders had no role in the design of the study; in the collection, analyses, or interpretation of data; in the writing of the manuscript, or in the decision to publish the results.

References

1. McMinn, P.C. An overview of the evolution of enterovirus 71 and its clinical and public health significance. *FEMS Microbiol. Rev.* **2002**, *26*, 91–107. [CrossRef] [PubMed]
2. Puenpa, J.; Wanlapakorn, N.; Vongpunsawad, S.; Poovorawan, Y. The History of Enterovirus A71 Outbreaks and Molecular Epidemiology in the Asia-Pacific Region. *J. Biomed. Sci.* **2019**, *26*, 75. [CrossRef]
3. Anasir, M.I.; Zarif, F.; Poh, C.L. Antivirals blocking entry of enteroviruses and therapeutic potential. *J. Biomed. Sci.* **2021**, *28*, 10. [CrossRef] [PubMed]
4. Baggen, J.; Thibaut, H.J.; Strating, J.R.P.M.; van Kuppeveld, F.J.M. The life cycle of non-polio enteroviruses and how to target it. *Nat. Rev. Microbiol.* **2018**, *16*, 391. [CrossRef] [PubMed]
5. Yeung, M.L.; Jia, L.; Yip, C.C.Y.; Chan, J.F.W.; Teng, J.L.L.; Chan, K.H.; Cai, J.P.; Zhang, C.; Zhang, A.J.; Wong, W.M.; et al. Human tryptophanyl-tRNA synthetase is an IFN-gamma-inducible entry factor for Enterovirus. *J. Clin. Investig.* **2018**, *128*, 5163–5177. [CrossRef]
6. Shingler, K.L.; Yoder, J.L.; Carnegie, M.S.; Ashley, R.E.; Makhov, A.M.; Conway, J.F.; Hafenstein, S. The enterovirus 71 A-particle forms a gateway to allow genome release: A cryoEM study of picornavirus uncoating. *PLoS Pathog.* **2013**, *9*, e1003240. [CrossRef]
7. Li, X.; Wang, M.; Cheng, A.; Wen, X.; Ou, X.; Mao, S.; Gao, Q.; Sun, D.; Jia, R.; Yang, Q.; et al. Enterovirus Replication Organelles and Inhibitors of Their Formation. *Front. Microbiol.* **2020**, *11*, 1817. [CrossRef]
8. Cao, J.; Liu, H.; Qu, M.; Hou, A.; Zhou, Y.; Sun, B.; Cai, L.; Gao, F.; Su, W.; Jiang, C. Determination of the cleavage site of enterovirus 71 VP0 and the effect of this cleavage on viral infectivity and assembly. *Microb. Pathog.* **2019**, *134*, 103568. [CrossRef]
9. Jacobson, M.F.; Baltimore, D. Morphogenesis of poliovirus: I. Association of the viral RNA with coat protein. *J. Mol. Biol.* **1968**, *33*, 369–378. [CrossRef]
10. Chandler-Bostock, R.; Mata, C.P.; Bingham, R.J.; Dykeman, E.C.; Meng, B.; Tuthill, T.J.; Rowlands, D.J.; Ranson, N.A.; Twarock, R.; Stockley, P.G. Assembly of infectious enteroviruses depends on multiple, conserved genomic RNA-coat protein contacts. *PLoS Pathog.* **2020**, *16*, e1009146. [CrossRef]
11. Curry, S.; Fry, E.; Blakemore, W.; Abu-Ghazaleh, R.; Jackson, T.; King, A.; Lea, S.; Newman, J.; Stuart, D. Dissecting the roles of VP0 cleavage and RNA packaging in picornavirus capsid stabilization: The structure of empty capsids of foot-and-mouth disease virus. *J. Virol.* **1997**, *71*, 9743–9752. [CrossRef] [PubMed]
12. Zhang, W.; Liu, H.T. MAPK signal pathways in the regulation of cell proliferation in mammalian cells. *Cell Res.* **2002**, *12*, 9–18. [CrossRef] [PubMed]
13. Pleschka, S. RNA viruses and the mitogenic Raf/MEK/ERK signal transduction cascade. *Biol. Chem.* **2008**, *389*, 1273–1282. [CrossRef] [PubMed]
14. Pleschka, S.; Wolff, T.; Ehrhardt, C.; Hobom, G.; Planz, O.; Rapp, U.R.; Ludwig, S. Influenza virus propagation is impaired by inhibition of the Raf/MEK/ERK signalling cascade. *Nat. Cell Biol.* **2001**, *3*, 301–305. [CrossRef] [PubMed]
15. Zhao, L.J.; Wang, W.; Liu, Y.; Ren, H.; Qi, Z.T. Interference with ERK and STAT signaling pathways and inhibition of hepatitis C virus replication by ribavirin. *Antivir. Res.* **2012**, *96*, 260–268. [CrossRef]
16. Luo, H.; Yanagawa, B.; Zhang, J.; Luo, Z.; Zhang, M.; Esfandiarei, M.; Carthy, C.; Wilson, J.E.; Yang, D.; McManus, B.M. Coxsackievirus B3 replication is reduced by inhibition of the extracellular signal-regulated kinase (ERK) signaling pathway. *J. Virol.* **2002**, *76*, 3365–3373. [CrossRef]
17. Wong, W.R.; Chen, Y.Y.; Yang, S.M.; Chen, Y.L.; Horng, J.T. Phosphorylation of PI3K/Akt and MAPK/ERK in an early entry step of enterovirus 71. *Life Sci.* **2005**, *78*, 82–90. [CrossRef]
18. Zhu, M.; Duan, H.; Gao, M.; Zhang, H.; Peng, Y. Both ERK1 and ERK2 are required for enterovirus 71 (EV71) efficient replication. *Viruses* **2015**, *7*, 1344–1356. [CrossRef]
19. Tung, W.H.; Hsieh, H.L.; Lee, I.T.; Yang, C.M. Enterovirus 71 modulates a COX-2/PGE2/cAMP-dependent viral replication in human neuroblastoma cells: Role of the c-Src/EGFR/p42/p44 MAPK/CREB signaling pathway. *J. Cell. Biochem.* **2011**, *112*, 559–570. [CrossRef]
20. Law, G.L.; Tisoncik-Go, J.; Korth, M.J.; Katze, M.G. Drug repurposing: A better approach for infectious disease drug discovery? *Curr. Opin. Immunol.* **2013**, *25*, 588–592. [CrossRef]
21. Pushpakom, S.; Iorio, F.; Eyers, P.A.; Escott, K.J.; Hopper, S.; Wells, A.; Doig, A.; Guilliams, T.; Latimer, J.; McNamee, C.; et al. Drug repurposing: Progress, challenges and recommendations. *Nat. Rev. Drug Discov.* **2019**, *18*, 41–58. [CrossRef]
22. Kim, G.; McKee, A.E.; Ning, Y.M.; Hazarika, M.; Theoret, M.; Johnson, J.R.; Xu, Q.C.; Tang, S.; Sridhara, R.; Jiang, X.; et al. FDA approval summary: Vemurafenib for treatment of unresectable or metastatic melanoma with the BRAFV600E mutation. *Clin. Cancer Res.* **2014**, *20*, 4994–5000. [CrossRef] [PubMed]
23. Kim, A.; Cohen, M.S. The discovery of vemurafenib for the treatment of BRAF-mutated metastatic melanoma. *Expert Opin. Drug Discov.* **2016**, *11*, 907–916. [CrossRef] [PubMed]
24. Ye, W.; Yao, M.; Dong, Y.; Ye, C.; Wang, D.; Liu, H.; Ma, H.; Zhang, H.; Qi, L.; Yang, Y.; et al. Remdesivir (GS-5734) Impedes Enterovirus Replication Through Viral RNA Synthesis Inhibition. *Front. Microbiol.* **2020**, *11*, 1105. [CrossRef]
25. Gordon, C.J.; Tchesnokov, E.P.; Woolner, E.; Perry, J.K.; Feng, J.Y.; Porter, D.P.; Gotte, M. Remdesivir is a direct-acting antiviral that inhibits RNA-dependent RNA polymerase from severe acute respiratory syndrome coronavirus 2 with high potency. *J. Biol. Chem.* **2020**, *295*, 6785–6797. [CrossRef]

26. Agostini, M.L.; Andres, E.L.; Sims, A.C.; Graham, R.L.; Sheahan, T.P.; Lu, X.; Smith, E.C.; Case, J.B.; Feng, J.Y.; Jordan, R.; et al. Coronavirus Susceptibility to the Antiviral Remdesivir (GS-5734) Is Mediated by the Viral Polymerase and the Proofreading Exoribonuclease. *mBio* **2018**, *9*, e00221-18. [CrossRef] [PubMed]
27. Chan, J.F.W.; Chik, K.K.H.; Yuan, S.F.; Yip, C.C.Y.; Zhu, Z.; Tee, K.M.; Tsang, J.O.L.; Chan, C.C.S.; Poon, V.K.M.; Lu, G.; et al. Novel antiviral activity and mechanism of bromocriptine as a Zika virus NS2B-NS3 protease inhibitor. *Antivir. Res.* **2017**, *141*, 29–37. [CrossRef] [PubMed]
28. Lu, J.; He, Y.Q.; Yi, L.N.; Zan, H.; Kung, H.F.; He, M.L. Viral kinetics of enterovirus 71 in human abdomyosarcoma cells. *World J. Gastroenterol.* **2011**, *17*, 4135–4142. [CrossRef] [PubMed]
29. Zhao, Z.; Li, Z.; Huan, C.; Liu, X.; Zhang, W. SAMHD1 Inhibits Multiple Enteroviruses by Interfering with the Interaction between VP1 and VP2 Proteins. *J. Virol.* **2021**, *95*, e0062021. [CrossRef]
30. Poulikakos, P.I.; Zhang, C.; Bollag, G.; Shokat, K.M.; Rosen, N. RAF inhibitors transactivate RAF dimers and ERK signalling in cells with wild-type BRAF. *Nature* **2010**, *464*, 427–430. [CrossRef]
31. Hatzivassiliou, G.; Song, K.; Yen, I.; Brandhuber, B.J.; Anderson, D.J.; Alvarado, R.; Ludlam, M.J.; Stokoe, D.; Gloor, S.L.; Vigers, G.; et al. RAF inhibitors prime wild-type RAF to activate the MAPK pathway and enhance growth. *Nature* **2010**, *464*, 431–435. [CrossRef] [PubMed]
32. Ianevski, A.; Yao, R.; Biza, S.; Zusinaite, E.; Mannik, A.; Kivi, G.; Planken, A.; Kurg, K.; Tombak, E.M.; Ustav, M., Jr.; et al. Identification and Tracking of Antiviral Drug Combinations. *Viruses* **2020**, *12*, 1178. [CrossRef]
33. Holzberg, M.; Boergeling, Y.; Schrader, T.; Ludwig, S.; Ehrhardt, C. Vemurafenib Limits Influenza A Virus Propagation by Targeting Multiple Signaling Pathways. *Front. Microbiol.* **2017**, *8*, 2426. [PubMed]
34. Nicolaides, T.; Nazemi, K.J.; Crawford, J.; Kilburn, L.; Minturn, J.; Gajjar, A.; Gauvain, K.; Leary, S.; Dhall, G.; Aboian, M.; et al. Phase I study of vemurafenib in children with recurrent or progressive BRAF(V600E) mutant brain tumors: Pacific Pediatric Neuro-Oncology Consortium study (PNOC-002). *Oncotarget* **2020**, *11*, 1942–1952. [CrossRef] [PubMed]
35. Van Tilburg, C.M.; Selt, F.; Sahm, F.; Bachli, H.; Pfister, S.M.; Witt, O.; Milde, T. Response in a child with a BRAF V600E mutated desmoplastic infantile astrocytoma upon retreatment with vemurafenib. *Pediatr. Blood Cancer* **2018**, *65*, e26893. [CrossRef]
36. Wang, C.Y.; Gao, L.Y.; Jin, Y.; Cardona, C.J.; Xing, Z. Regulation of host responses and viral replication by the mitogen-activated protein kinases in intestinal epithelial cells infected with Enterovirus 71. *Virus Res.* **2015**, *197*, 75–84. [CrossRef]
37. Wang, C.; Zhou, R.; Zhang, Z.; Jin, Y.; Cardona, C.J.; Xing, Z. Intrinsic apoptosis and proinflammatory cytokines regulated in human astrocytes infected with enterovirus 71. *J. Gen. Virol.* **2015**, *96*, 3010–3022. [CrossRef]
38. Laajala, M.; Reshamwala, D.; Marjomaki, V. Therapeutic targets for enterovirus infections. *Expert Opin. Ther. Targets* **2020**, *24*, 745–757. [CrossRef]
39. Wang, R.Y.; Kuo, R.L.; Ma, W.C.; Huang, H.I.; Yu, J.S.; Yen, S.M.; Huang, C.R.; Shih, S.R. Heat shock protein-90-beta facilitates enterovirus 71 viral particles assembly. *Virology* **2013**, *443*, 236–247. [CrossRef]
40. Tsang, J.O.; Zhou, J.; Zhao, X.; Li, C.; Zou, Z.; Yin, F.; Yuan, S.; Yeung, M.L.; Chu, H.; Chan, J.F. Development of Three-Dimensional Human Intestinal Organoids as a Physiologically Relevant Model for Characterizing the Viral Replication Kinetics and Antiviral Susceptibility of Enteroviruses. *Biomedicines* **2021**, *9*, 88. [CrossRef]
41. Zou, Z.; Tsang, J.O.; Yan, B.; Chik, K.K.; Chan, C.C.; Cao, J.; Liang, R.; Tang, K.; Yin, F.; Ye, Z.W.; et al. Metabolic Profiling Reveals Significant Perturbations of Intracellular Glucose Homeostasis in Enterovirus-Infected Cells. *Metabolites* **2020**, *10*, 302. [CrossRef]
42. Hu, B.; Siche, S.; Moller, L.; Veit, M. Amphipathic Helices of Cellular Proteins Can Replace the Helix in M2 of Influenza A Virus with Only Small Effects on Virus Replication. *J. Virol.* **2020**, *94*, e01605-19. [CrossRef] [PubMed]